Theor Chem Acc (2003) 109:332–340
DOI 10.1007/s00214-003-0441-7

Theoretical
Chemistry Accounts

Regular article

Why are hexavalent uranium cyanides rare while U–F and U–O bonds are common and short?

Michal Straka[1,2], **Michael Patzschke**[1], **Pekka Pyykkö**[1]

[1]Department of Chemistry, University of Helsinki, POB 55 (A. I. Virtasen aukio 1), -00014 Helsinki, Finland
[2]*Present address*: Institut für Anorganische Chemie, Universität Würzburg, Am Hubland, D-97074 Würzburg, Germany

Received: 23 October 2002 / Accepted: 19 January 2003 / Published online: 20 May 2003

Abstract. Relativistic small-core pseudopotential B3LYP and CCSD(T) calculations and frozen-core PW91–PW91 studies are reported for the series UF_4X_2 (X = H, F, Cl, CN, NC, NCO, OCN, NCS and SCN). The bonding in UF_6 is analyzed and found to have some multiple-bond character, approaching at a theoretical limit a bond order of 1.5. In addition to these σ and π orbital interactions, the electrostatic attraction is important. Evidence for π bonding in the other systems studied was also found. The triatomic pseudohalides as well as fluorine and chlorine are in this sense better ligands than cyanide. The –CN group is a σ donor and π acceptor, as uranium itself, and hence is unfit to bond to U(VI). The σ-bonded UH_6 is octahedral.

Keywords: Uranium – Transition-metal complexes – Uranium hexafluoride

1 Introduction

The pseudohalide cyanide, CN^-, is a stable moiety, often interchangeable with chloride or other halides. It forms binary compounds with the *s*, *p*, and *d* metals. Both alkali cyanides and the d^{10} gold dicyanide anion $Au(CN)_2^-$ are well-known examples. Against this background it is interesting that uranium cyanides are rare. In fact, no d^0f^0 $U(CN)_6$ or $U(NC)_6$ seem to be known. Uranium carbonyls $U(CO)_n$, n = 1–6 are known [1, 2], but have formally U(0), not U(VI), and cannot hence be compared with the cyanides. There exist tertiary cyanides for lower oxidation states of uranium, such as $U(cp)_3CN$ [3, 4], (cp = C_5H_5), which is believed to have an oligomeric structure with –CN–U–CN–U–CN– chains, where uranium is in a trigonal bipyramidal position. The structure of $UCl_3CN{\cdot}4NH_3$ [5] is not known but its spectroscopic properties suggest a similar chain. Bagnall and Baptista [5] stated that actinide (IV) cyanides would have been of considerable spectroscopic interest, but could not be obtained by reaction of the tetrachloride with alkali-metal cyanides in liquid hydrogen cyanide. Solid-state systems in which uranium is linked through cyanide nitrogen to $M(CN)_4^{2-}$ units (M = Ni, Pt) [6], $M(CN)_6^{4-}$ units (M = Fe, Ru) [7, 8], and $M(CN)_8^{4-}$ units (M = Mo, W) [7, 8] are known experimentally. On the other, there exist a number of uranium species with –NCS or –SCN ligands. Also uranium species with an –NCO ligand [9, 10] and with –CN–*R* or –NC–*R* ligands exist, see Ref. [11] for recent examples. We are not aware of any systems with a U–OCN bond.

Why are the cyanides of uranium rare and why in the species with a linking CN group to another metal does the nitrogen always links to uranium? Why are then the species of uranium with triatomic pseudohalides, particularly isothiocyanide, rather more numerous? We try to answer these questions in the present work, concentrating on the oxidation state VI of uranium. Several systems, derived from the well-known UF_6, the *trans*– and *cis*–UF_4X_2 (X = Cl, CN, NC, NCS, SCN, NCO, OCN) were calculated, using several methods. The UF_4X_2 systems were chosen for computational economy instead of the more symmetric UX_6 systems. Apart from the species with X = F, Cl these systems have not been reported experimentally. The single-molecule structures, frequencies, thermodynamic stabilities and bonding are compared and discussed. UF_6 [12] and UF_4Cl_2 [13] are known molecules and serve as reference points. In fact, we present evidence that the important UF_6 itself may possess some multiple-bonding character.

2 Methods

Studies on actinide species showed that density functional methods with effective core potentials (ECP) give reasonable results for actinide systems [14, 15, 16, 17, 18, 19, 20, 21, 22]. We used the B3LYP functional [23,24] and the TZVP basis set for C, N, O, F, S and Cl atoms [25]. The relativistic small-core ECP with the corresponding basis set [26, 27] was used for uranium. Single-point

---

Correspondence to: Pekka Pyykkö
e-mail: pekka.pyykko@helsinki.fi

CCSD(T) calculations were done as a reliability check. The B3LYP and CCSD(T) calculations as well as the frequency calculations were done with the Gaussian 98 software package [28].

The systems were closed-shell, formally f^0d^0 species. Therefore spin–orbit corrections are expected to be small and were not considered. It is difficult to obtain an initial wavefunction for actinide species. We altered the initial extended Hückel guess and checked the stability of the wavefunction via the tools available in Gaussian 98 [28]. The principles of the natural bond orbital (NBO) analysis are described in Ref. [29].

Further calculations were done using the ADF2000 software package [30, 31, 32]. The zero-order regular approximation was employed in all ADF calculations. This was done because, owing to singularities at the nucleus in the Pauli–Hamiltonian, the use of this model for actinide species is not advisable. As the local density approximation part of the exchange functional we chose VWN [33] and for the generalised gradient approximations part PW91 [34]. For the correlation part we also chose PW91. The ADF package uses Slater-type orbitals instead of Gaussian-type orbitals as used in Gaussian 98. That makes a direct comparison of the basis sets somewhat difficult. We used the ADF2000 type IV basis set. This is of TZP quality. We used the frozen-core approach as implemented in ADF to describe the inner electrons of uranium. All electrons up to $5d$ were considered as frozen, the remaining 14 electrons constituted the active part. The fragment analysis was also done with ADF; the method is described in some detail in Refs. [35, 36, 37].

3 Results and discussion

3.1 Bonding in UF_6

We start our discussion from an analysis of uranium hexafluoride, studied in numerous earlier papers, see Refs. [14, 17, 38, 39, 40, 41, 42] and references therein. In the 36-valence-electron picture (F $2p^5$, U $5f^3 6d^1 7s^2$) it corresponds to an

$$e_g^4 + t_{2g}^6 + 1t_{1u}^6 + a_{1g}^2 + t_{2u}^6 + t_{1g}^6 + 2t_{1u}^6 \qquad (1)$$

orbital structure. These orbitals, plotted with Molden [43], are shown in Fig. 1 and their character is discussed in Table 1. Now, if the fluorines acted as σ acceptors only, their $2p\sigma$ orbitals would span the $a_{1g} + e_g + t_{1u}$ symmetry orbitals, corresponding to six single bonds to the uranium $7s$, $6d$ and $5f$ orbitals, respectively. In addition, we note, however, a conspicuous donation from the filled F $2p\pi$ to the U $5f$ and $6d$ parts of the bonding t_{2u} (HOMO-2) and t_{2g} (HOMO-5) orbitals. The σ and π t_{1u} combine to a bonding $1t_{1u}$ and antibonding $2t_{1u}$. Altogether this gives 12 bonding, three antibonding

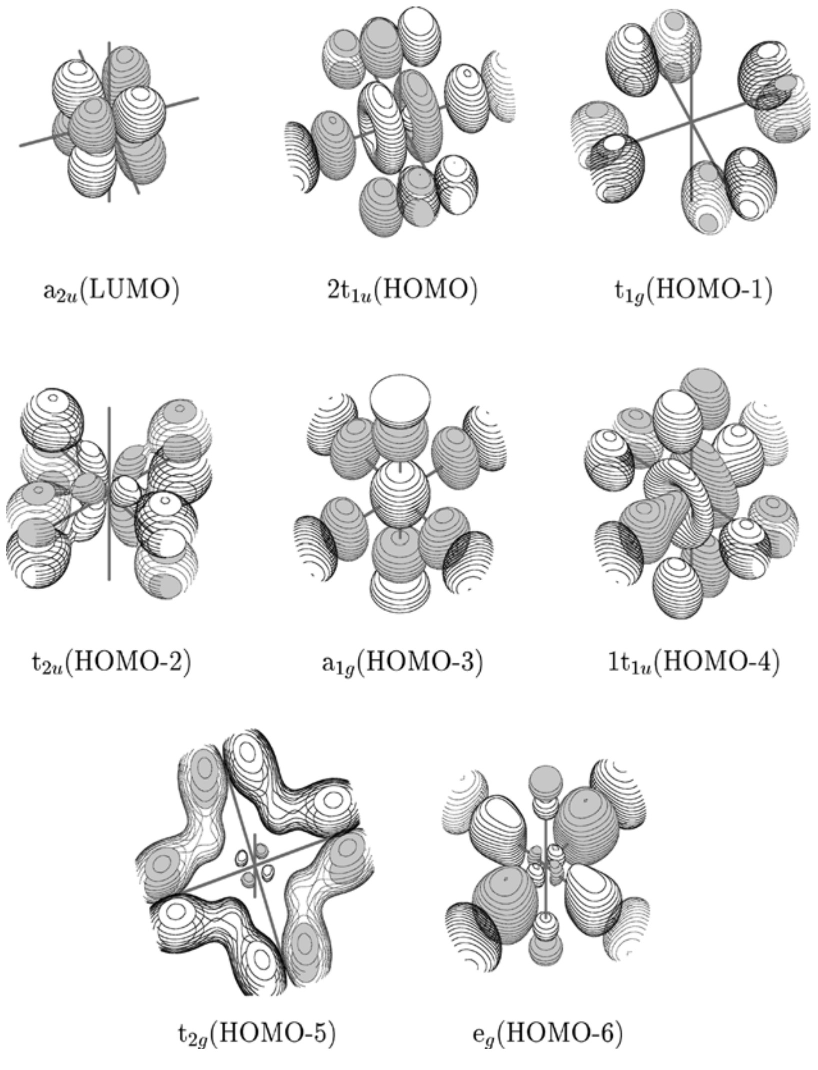

Fig. 1. Isodensity plot of the B3LYP molecular orbitals of UF_6 calculated with Gaussian98 and plotted with Molden

Table 1. The chemically relevant molecular orbitals of UF_6 and their qualitative atomic orbital character at U and F. For the orbital shapes see Fig. 1

MO		U	F	Comments
a_{2u}	LUMO	f_{xyz}	–	
$2t_{1u}$	HOMO	[a]	$2p\sigma + 2p\pi$	Antibonding to 5*f*
t_{1g}	HOMO-1	–	$2p\pi$	Nonbonding
t_{2u}	HOMO-2	[a]	$2p\pi$	Bonding
a_{1g}	HOMO-3	$7s$	$2p\sigma$	Bonding
$1t_{1u}$	HOMO-4	[a]	$2p\sigma + 2p\pi$	Bonding to 5*f*
t_{2g}	HOMO-5	$6d_{xy}$	$2p\pi$	Bonding
e_g	HOMO-6	$6d_{x^2-y^2}$	$2p\sigma$	Bonding

[a] The t_{1u} basis is $[(5z^3 - 3zr^2), (5y^3 - 3yr^2), (5x^3 - 3xr^2)]$, The t_{2u} basis is $[x(z^2 - y^2), y(z^2 - x^2), z(x^2 - y^2)]$

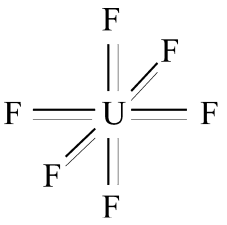

Fig. 2. A symbolic description for the partial multiple bonding of UF_6

and three nonbonding orbitals. A simple subtraction gives a theoretical maximum bond order of (12-3 + 0.3)/6 = 1.5, with a clear multiple-bonding character as symbolically presented in Fig. 2. Note the contrast to the *d*-element hexahalides, such as CrF_6 or WF_6, which could only have covalent bonding to gerade orbitals (apart from small np contributions), $a_{1g} + e_g + t_{2g}$ [44], corresponding at most to a single bond. The actinides can also bond to the ungerade 5*f*.

Parenthetically, one should note that just as the carbon atom in carbon monoxide, $\sigma^2\pi^4$, can have a triple C≡O bond to the oxygen atom, nothing prevents a fluorine atom from having multiple-bond character in a compound, should that correspond to the actual molecular orbital (MO) structure of the compound. Examples involving fluorine are the O = C = O isoelectronic analogs FCF^{2+} [45], FBF^+, FNF^{3+}, and NNF^+ [46]; the latter system was discussed from the point of view of interatomic repulsion by Bickelhaupt et al. [47]. A triple-bond character is generally accepted for uranyl, up to the theoretical limit of $\sigma_g^2\sigma_u^2\pi_g^4\pi_u^4$, $O{\equiv}U{\equiv}O^{2+}$ [38,48] but we are not aware of earlier discussions of any multiple-bond character in UF_6.

Thus, in UF_6, U^{6+} was a good σ donor, when giving away its six valence electrons to fluorine, and remains a good π acceptor. Inversely, F^- was a good σ acceptor while accepting the extra electron, and is now a good π donor. This leads to a perfect match. In addition, there will be an ionic component to the bonding.

3.1.1 Nature of bonding

The contributions to the bonding in UF_6 from a fragment analysis as implemented in ADF are shown in Table 2. It is seen that orbital interactions are almost as important as the electrostatic ("steric") ones and that, in the former, the π-orbital interactions play an important role. Electrostatics is not enough, and covalent σ bonding is not enough.

Table 2. Fragment analysis (results obtained with ADF using the PW91–PW91 combination of functionals, see Sect. 2) for *trans*-UF_4X_2, (X = F, Cl, CN, NC, NCS, SCN, NCO, OCN). The fragments are $UF_4^{2+} + 2X^-$. $UF_4(SCN)_2$ is a transition state in D_{4h} symmetry. All values are in eV. Note that two bonds are substituted. The symmetry labels are in D_{4h}

	UF_6	UF_4Cl_2	$UF_4(CN)_2$	$UF_4(NC)_2$	$UF_4(NCS)_2$	$UF_4(SCN)_2$	$UF_4(NCO)_2$	$UF_4(OCN)_2$
Steric interaction								
Pauli repulsion	16.0725	12.0424	12.0309	12.3421	12.1762	6.1948	13.8889	8.7994
Electrostatic interaction[a]	−33.5916	−26.3547	−26.8905	−26.5966	−24.3363	−16.0957	−27.711	−21.312
Total steric interaction	−17.5192	−14.3122	−14.8595	−14.2546	−12.1601	−9.9008	−13.8225	−12.5126
Orbital interactions								
$a_{1g}(\sigma)$[b]	−1.9395	−2.3666	−2.2752	−1.9641	−1.9616	−1.7877	−2.0109	−1.6156
a_{2g}	−0.0222	−0.0152	−0.0132	−0.0133	−0.0124	−0.0066	−0.0155	−0.0111
b_{1g}	−0.0598	−0.0395	−0.0379	−0.0372	−0.0350	−0.0142	−0.0429	−0.0292
$b_{2g}\ (\pi)$	−0.0506	−0.0327	−0.0331	−0.0319	−0.0296	−0.0104	−0.0367	−0.0245
$e_{1g}(\pi)$	−2.0091	−1.8856	−1.1213	−1.7856	−2.5791	−2.3881	−2.4784	−2.2904
a_{1u}	0.0000	0.0000	0.0000	0.0000	0.0000	0.0000	0.0000	0.0000
$a_{2u}(\sigma + \pi)$	−3.5231	−2.7018	−2.8832	−2.7319	−1.9837	−0.9778	−2.1611	−1.4663
b_{1u}	0.0000	0.0000	0.0000	0.0000	0.0000	0.0000	0.0000	0.0000
$b_{2u}(\pi)$	−0.1835	−0.1201	−0.1395	−0.1286	−0.1348	−0.0367	−0.1477	−0.1017
$e_{1u}(\pi \text{ and } \sigma + \pi)$	−3.2359	−3.0682	−2.1034	−2.7185	−5.0000	−5.3656	−4.2256	−4.5360
Total orbital interactions	−11.0236	−10.2296	−8.6068	−9.4111	−11.7362	−10.5872	−11.1188	−10.0747
Total bonding energy	−28.5428	−24.5418	−23.4664	−23.6657	−23.8962	−20.4881	−24.9413	−22.5874

[a] The electrostatic interaction includes the fit correction

[b] Qualitative character of the ligand orbitals involved (see also Table 1)

Table 3. The valence natural atomic orbital occupancies [σ is $2(3)s + 2(3)p_z$ and π is $2(3)p_x + 2(3)p_y$] for the *trans*-UF_4X_2 (X = F, Cl, CN, NC, NCS, NCO, OCN) and the X^- (X = CN, NCS, NCO) systems

X	U(5f, 6d, 7s)	F(σ)	F(π)	N(σ)	N(π)	C(σ)	C(π)	O/S/Cl (σ)	O/S/Cl (π)	$\sigma(X)$	$\pi(X)$
UF_6	2.41, 0.42, 0.11	3.75	3.76								
trans-UF_4Cl_2	2.67, 0.50, 0.19	3.81	3.68					3.64	3.68	3.64	3.68
trans-$UF_4(CN)_2$	2.46, 0.40, 0.22	3.81	3.67	3.12	2.10	2.38	1.80			5.50	3.90
trans-$UF_4(NC)_2$	2.47, 0.22, 0.15	3.81	3.66	3.02	2.84	2.61	0.98			5.63	3.82
trans-$UF_4(NCS)_2$	2.58, 0.22, 0.15	3.81	3.69	2.96	2.74	1.98	1.80	2.80	3.04	7.74	7.54
trans-$UF_4(NCO)_2$	2.56, 0.39, 0.15	3.82	3.68	2.93	2.89	1.57	1.57	3.23	3.19	7.73	7.65
trans-$UF_4(OCN)_2$	2.54, 0.39, 0.12	3.81	3.68	3.07	2.25	1.57	1.85	3.19	3.49	7.83	7.59
CN^-				3.20	2.51	2.70	1.48			5.90	3.99
NCS^-				3.10	2.44	1.99	1.92	2.84	3.60	7.94	7.96
NCO^-				3.09	2.69	1.62	1.79	3.24	3.49	7.95	7.97

Table 4. Natural charges for the *trans*–UF_4X_2 (X = F, Cl, CN, NC, NCS, NCO, OCN, SCN) and X^- (X = CN, NCS, NCO) systems at B3LYP level

System	U	F	N	C	O/S/Cl	X (total)
UF_6	+3.05	−0.51				−0.51
trans-UF_4Cl_2	+2.64	−0.50			−0.33	−0.33
trans-$UF_4(CN)_2$	+2.98	−0.49	−0.26	−0.25		−0.51
trans-$UF_4(NC)_2$	+3.04	−0.48	−0.92	+0.36		−0.56
trans-$UF_4(NCS)_2$	+2.92	−0.52	−0.73	+0.16	+0.14	−0.43
trans-$UF_4(NCO)_2$	+2.94	−0.50	−0.85	+0.82	−0.43	
trans-$UF_4(OCN)_2$	+2.97	−0.49	−0.34	+0.54	−0.70	−0.50
trans-$UF_4(SCN)_2$	+2.67	−0.52	−0.25	+0.01	−0.04	−0.30
CN^-			−0.75	−0.25		−1.00
NCS^-			−0.57	+0.03	−0.46	−1.00
NCO^-			−0.80	+0.54	−0.74	−1.00

We also carried out a NBO analysis for UF_6, see Tables 3 and 4. The natural charges for UF_6 are +3.05 on U and −0.51 on F, consistent with a polar but not completely ionic character of the U–F bond. The natural atomic orbital (NAO) population of the fluorine $2p\pi$ lone pairs is 3.76 electrons. The natural localized MO (NLMO) analysis shows six σ U–F bonds with 13% U and 87% F character, and 12 fluorine lone pairs with "tails" at uranium d and f shells, having 94% F and 6% U character. This provides further evidence for the π bonding in UF_6. We show in Fig. 3 the density differences between the molecule and spherically averaged atoms at the covalent and ionic limits. The light-grey areas represent regions with increased electron density in the molecule. From Fig. 3 a it is obvious that electron density has been transferred from uranium f orbitals to the U–F bonds. There is also a shift in electron density from the p_z orbitals of fluorine to p_x and p_y orbitals, making the fluorine better suited to π bonding. From Fig. 3 b it can be seen that electron density from F^- is transferred to U^{6+} and that this density comes mainly from p_z orbitals of fluorine. This leaves electron density at p_x and p_y, enabling π bonding to uranium. These local density increases could, in principle, be observed experimentally.

In an early discussion of ionic and covalent character of U–F bonds in complex fluorides, Ohwada [49] set the UF_6 bond as 100% covalent.

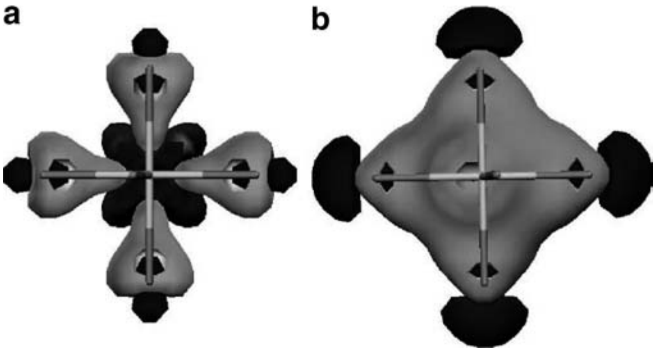

Fig. 3. Electron density difference between UF_6 and spherically averaged atoms calculated with ADF at PW91–PW91 level and plotted with Molekel [64]. **a** U + 6 F, **b** U^{6+} + 6 F^-. Cut through a UF_4 plane

3.1.2 Oxophilicity of uranium

The character of the strong U≡O bonds of uranyl was already discussed. From UF_6 we can now move to U–O–X bonds, noting that O and F are neighbours in the periodic table. For U–F distances, see Table 5. The U–O distances in $U(OX)_6$ are 210 and 205(2) pm and the U–O–X angles 136–140° and 170–171° for X = CH_3 (calculations by Schreckenbach [50]) and X = TeF_5 (X-ray data of Templeton et al. [51]), respectively. These U–O distances are only slightly larger than the U–F one in UF_6. The large U–O–X angles also suggest some π bonding. Such multiple-bond character was suspected as long ago as in 1981 by Cuellar and Marks [52] on the basis of ^{19}F NMR chemical shifts in the $U(OCH_3)_nF_{6-n}$ species. If the ligand $2p\pi$ donor ability becomes an important factor, one also understands why, in the heteronuclear NUO^+ system, the N–U bond is the shorter one [38, 53] and in the CUO system, the C–U bond is the shorter one [2, 38]. Here the electrostatic interaction would make the U–O bond shorter, because C and N are less electronegative than O.

3.2 UH_6

No π bonding is expected in U–H bonds; thus UH_6 would roughly simulate UF_6 ("with σ bonds only". It

Table 5. The calculated structures for the UF_4X_2 (X = F, Cl, CN, NC, NCS, NCO, OCN, SCN) and X^- (X = CN, NCS, NCO) systems, at density functional theory level. Distances in pm, angles in degrees (whenever angles are not reported, they correspond to intuitive quasi-O_h or D_{4h} symmetry)

System	Method	U–F[a]	U–X	C–N	C = O/S	FUF[a]	X_1UX_1[b]	UX_1X_2[b]	$X_1X_2X_3$[b]
UF_6	B3LYP	201.2							
	[c]	202.5							
	Exp.[d]	199.6 (8)							
trans-UF_4Cl_2	B3LYP	200.5	248.9						
	[c]	202.1	250.6						
cis-UF_4Cl_2	B3LYP	200.6, 200.8	248.6				90.5		
	[c]	201.9, 202.5	250.3						
trans-$UF_4(H)_2$	PW91-PW91[e]	202.0	193.6						
trans-$UF_4(CN)_2$	B3LYP	199.1	234.8	116.3					
cis-$UF_4(CN)_2$	B3LYP	199.0, 199.9	234.1	116.3		173.5, 93.4	88.0	179.4	
trans-$UF_4(NC)_2$	B3LYP	199.7	221.0	119.0					
cis-$UF_4(NC)_2$	B3LYP	199.8, 200.8	219.7	119.0		178.2, 91.2	88.9	179.8	
trans-$UF_4(NCS)_2$	B3LYP	202.0	218.9	120.3	157.4				
cis-$UF_4(NCS)_2$	B3LYP	202.0, 202.9	217.2	120.4	157.2	179.4, 92.4	87.4	171.8	179.5
trans-$UF_4(NCO)_2$	B3LYP	201.7	215.9	121.2	116.5				
cis-$UF_4(NCO)_2$	B3LYP	201.7, 202.5	214.7	121.3	116.4	179.7, 91.2	88.9	172.4	179.5
trans-$UF_4(OCN)_2$	B3LYP	200.6	212.6	116.4	126.3				
cis-$UF_4(OCN)_2$	B3LYP	200.5, 201.6	211.7	116.3	126.5	179.0, 92.6	88.9	168.8	179.7
trans-$UF_4(SCN)_2$	B3LYP	200.4	266.4	116.1	168.7		180.0	97.2	178.6
trans-$UF_4(SCN)_2$	PW91-PW91[e]	201.1, 201.3	267.7	117.3	167.1		180.0	96.4	178.9
cis-$UF_4(SCN)_2$	PW91-PW91[e]	201.5, 201.6	269.5	117.3	166.8	176.8, 91.3	119.6	106.1	176.2
CN^-	B3LYP			117.4					
NCS^-	B3LYP			117.5	166.9				
NCO^-	B3LYP			118.9	122.9				

[a] The first value is for the fluorine(s) cis to X(s), the second for the fluorine(s) trans to X

[b] X_1 is the first atom bonded to U and X_2 and X_3 the second and third atoms of U, respectively

[c] Ref. [50]

[d] Ref. [63]

[e] Optimized with ADF

Table 6. Structure and harmonic frequencies of UH_6 calculated with B3LYP, PW91–PW91 and Dirac–Fock one-centre expansion (as computed by Pyykkö and Desclaux in 1978 [54]) (*DF-OCE*). Distances in pm, frequencies in cm^{-1} and IR intensities in km mol^{-1}

	B3LYP	PW91VWN	DF-OCE
Bond length	195.7	196.7	198.0
Frequencies (Intensities)			
a_{1g}	1620.0 (0)	1571.2 (0)	1689
t_{1u}	1534.0 (660)	1502.2 (581)	
e_g	1449.0 (0)	1450.9 (0)	
t_{2g}	510.0 (0)	511.3 (0)	
t_{1u}	399.0 (163)	394.0 (161)	
t_{2u}	367.0 (0)	349.0 (0)	

was treated earlier assuming octahedral symmetry [54]. We now verify the octahedral symmetry, as shown by the real frequencies in Table 6. If the f basis functions for U are omitted, the molecule distorts to C_{3v} symmetry. Then it would resemble the experimentally known WH_6, which has a distorted trigonal prism structure [55].

Experimentally, UH_n species with $n = 1$–4 were made in matrices by Souter et al. [56]. The reaction $UH_4(S = 1, T_d) + H_2 \rightarrow UH_6$ was calculated by us to be endothermic by 2.48 eV, explaining why UH_6 was not seen by them.

3.3 UF_4X_2

3.3.1 Structures

The calculated B3LYP structures of the UF_4X_2 (X = Cl, CN, NC, NCS, SCN, NCO, OCN) molecules are shown in Table 5. The calculated ADF structures were very similar. Both the UF_6 and UF_4Cl_2 results are compared with these of earlier calculations [41,50] in Table 5. All trans systems have a D_{4h} symmetry, except $UF_4(SCN)_2$, whose U–S–C angles were not linear. The angles in *cis* systems are close to those of pseudo-octahedral symmetry. U–X bond distances are longer in all trans isomers, compared to the cis isomers. In cis isomers, the U–F distances are longer for fluorines trans to X. The X_1–U–X_1 angles in cis isomers (X_1 is a ligand atom bonded to uranium) are close to 90°, triatomic ligands bend away from each other, remaining close to linear, see the UX_1X_2 angles in Table 5. The fluorines out of the X–U–X plane (in cis systems) bend towards the diagonal of the X_1–U–X_1 angle. This is pronounced for $X = CN$ and suggests some interaction of F $2p\pi$ and antibonding CN π^* orbitals.

3.3.2 Energies

The energy differences between cis and trans structures are small (see supplementary material). From now on we shall therefore concentrate on the trans systems. In Table 7 we give the hypothetical gas-phase formation

Table 7. The B3LYP [CCSD(T)] calculated energies for selected reactions. R1: $UF_6 + X_2 = UF_4X_2 + F_2$; R2: $UF_6 + 2HX = UF_4X_2 + 2HF$; R3: $UF_6 + 2X^- = UF_4X_2 + 2F^-$ (X = F, Cl, CN, NC, NCS, NCO, OCN, SCN). In kJ mol^{-1}

X	Product	R1	R2	R3
Cl	*trans*-UF_4Cl_2	369.8 (330.3)	33.5 (4.0)	399.2 (339.3)
CN	*trans*-$UF_4(CN)_2$	802.0 (760.2)	317.5 (276.7)	530.3 (518.1)
NC	*trans*-$UF_4(NC)_2$	777.5 (745.5)	293.0 (262.0)	505.8 (503.3)
NCS	*trans*-$UF_4(NCS)_2$	391.4	71.9 (25.7)	512.7 (509.9)
NCO	*trans*-$UF_4(NCO)_2$	390.0	82.2	391.9
OCN	*trans*-$UF_4(OCN)_2$	587.9	280.1	589.7
SCN	*trans*-$UF_4(SCN)_2$	591.3	247.0	687.8

energies (at B3LYP level without zero-point energies) for the trans systems studied and model reactions starting from UF_6 and either X_2(R1), H–X(R2), or X^-(R3). In addition to the inherent stability of the UF_4X_2 species, the reaction energies in Table 7 are influenced by other factors: The strength of the X–X bond for reaction R1, that of the H–X bond for reaction R2, and the formation energy of the X^- ions for reaction R3. Nevertheless, two trends can be observed: bonding through the nitrogen end is energetically favoured, and triatomic pseudohalides NCS and NCO are favoured over the cyanide and are energetically close to chlorine.

3.3.3 Fragment analysis

These total-energy conclusions are fully supported by the fragment analysis in Table 2. The U–F bond is the strongest one in the table and derives its unique strength from a strong ionic attraction, on top of the orbital interaction. The U–Cl bonds have orbital interactions about 0.8 eV weaker than the U–F ones, owing to a stronger a_{1g} σ bond but weaker π bonds. Going from Cl to cyanide and isocyanide, the "steric" parts are comparable, but both cyanides have weaker orbital interactions. Indeed, cyanide is a splendid σ donor and a reasonable π acceptor, and is hence an anathema to U(VI). Also here the isocyanide forms a better bond than the cyanide. The NCS and NCO ligands form stronger bonds to U(VI) than the cyanides, mainly due to strong orbital interactions. Notably, the e_{1u} contribution is strong. The oxygen end of cyanate is worse than the nitrogen end. Half of the difference is steric, the other half coming from orbital interactions. The sulphur end of –SCN is worse than the nitrogen end, a third of the difference coming from orbital interactions and the rest from the steric part.

As a further, qualitative discussion we can sketch the MOs of the cyanides, as shown in Fig. 4. In its bonding the carbon $2p\pi$ orbital can receive a larger coefficient upon diagonalization of the M–CN π system. Such an increase is tantamount to π back-bonding, known from common textbooks. It will lead to a strengthening of the M–CN bond, weakening of the C–N bond, and a decrease of the metal $d\pi$ character for d transition metals. It is symptomatic that no cyanides seem to exist for the lighter transition metals in their highest d^0 oxidation states, either [57].

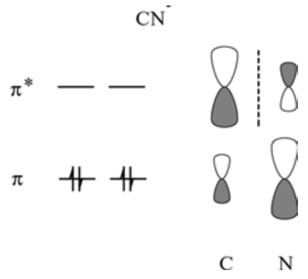

Fig. 4. Schematic diagram of the π orbitals of CN^-

With d^0f^0 actinides, like U(VI), the situation differs from the d^n metals. Originally, the metal ion has no valence electrons and is a good π acceptor, preferring the nitrogen end of the cyanide, which is a good π donor. This overrides the less advantageous σ bonding at the nitrogen end of cyanide. Even in the mixed uranium (IV) transition-metal cyanide species, mentioned in the Introduction, the nitrogen is always bonded to uranium and the carbon to a transition metal.

3.3.4 Population analysis

The data in Table 4 show for all ligands similar total natural charges of -0.5 ± 0.1, except -0.33 for Cl. In polyatomic ligands, if the first atom, X_1, is nitrogen it carries a high negative charge of -0.83 ± 0.10. The U–Cl bond is less polar than the U–F bond, as might be expected. The NAO population of chlorine $3p\pi$ lone pairs is 3.68. The NLMO analysis shows 4 σ U–F bonds (13% U, 87% F) and 2 σ U–Cl bonds (8% U, 92% Cl). The $2p\pi$ and $3p\pi$ lone pairs of F and Cl have "tails" at uranium d and f shells with 6% U and 94% F character and 19% U and 81% Cl, respectively. Thus neither the U–F nor the U–Cl bond can be regarded as a pure σ bond.

3.3.5 Frequencies

In d transition-metal cyanides the π back-bonding is reflected as a decrease of the CN stretching frequency. The same trend is expected and observed here for direct π bonding. The calculated vibrational frequencies are shown in Tables 8 and 9. In *trans*–UF_4X_2 species the CN stretch combines to symmetric and antisymmetric vibration, see first and second rows of Tables 8 and 9. The calculated value for free CN^- stretching of 2135 cm^{-1} decreases to 2045 and 2026 cm^{-1} in $UF_4(NC)_2$ and increases to 2229 and 2232 cm^{-1} in $UF_4(CN)_2$. The same is valid for $UF_4(NCS)_2$, where the CN stretch is decreased from 2143 cm^{-1} in the free thiocyanide anion to 1992 and 1973 cm^{-1} in the complex. However, for $UF_4(NCO)_2$, the CN stretch increases on complexation (though the bond is longer). Thus the situation is more complex in the triatomic ligands.

Table 8. Calculated harmonic frequencies and corresponding IR intensities (in *parentheses*) for the systems studied. In cm^{-1} and km mol^{-1}. Free-ion frequencies: σ(CN$^-$) 2135(11), σ(SCN$^-$) 2144(336) and 730(11), π(SCN$^-$) 481(3), σ(NCO$^-$) 2215(640) and 1251(55), π(NCO$^-$) 642(12) cm^{-1}

trans-UF$_4$Cl$_2$		*cis*-UF$_4$Cl$_2$		*trans*-UF$_4$(CN)$_2$		*cis*-UF$_4$(CN)$_2$		*trans*-UF$_4$(NC)$_2$		*cis*-UF$_4$(NC)$_2$	
e_u	611 (203)	a_1	634 (148)	a_{1g}	2229	a_1	2221 (132)	a_{1g}	2045	a_1	2043 (543)
a_{1g}	607	b_1	610 (205)	a_{2u}	2232 (376)	b_2	2216 (219)	a_{2u}	2026 (1619)	b_2	2014 (897)
b_{1g}	532	b_2	575 (109)	e_u	632 (197)	a_1	644 (136)	e_u	624 (203)	a_1	633 (154)
a_{2u}	351 (134)	a_1	548 (21)	a_{1g}	622	b_1	631 (197)	a_{1g}	616	b_1	622 (204)
a_{1g}	317	a_1	342 (42)	b_{1g}	547	b_2	587 (113)	b_{1g}	540	b_2	580 (130)
b_{2g}	199	b_2	323 (54)	a_{2u}	362 (145)	a_1	564 (29)	a_{2u}	409 (221)	a_1	557 (34)
a_{2u}	178 (7)	b_1	195 (5)	a_{1g}	335	a_1	356 (47)	a_{1g}	381	a_1	409 (63)
e_g	165	a_1	188 (7)	e_u	234	b_2	342 (57)	e_g	204	b_2	385 (84)
e_u	159 (7)	a_2	185	e_g	221	a_2	234 (0)	b_{2g}	198	a_2	203
b_{2u}	136	b_2	168 (7)	b_{2u}	199	b_1	232 (1)	e_u	185 (6)	b_1	201
e_u	94	a_1	153 (2)	e_u	154 (8)	a_1	209 (2)	a_{2u}	164 (10)	a_1	201
		b_1	139 (3)	a_{2u}	143 (10)	b_2	200 (0)	e_u	145 (3)	b_1	180 (9)
		b_2	122	a_{2g}	104	b_1	181 (6)	b_{2u}	123	b_2	176 (7)
		a_2	107	b_{2u}	104	a_2	166 (0)	e_g	84	a_1	172 (10)
		a_1	106	e_u	60 (6)	a_1	163 (8)	e_u	57 (3)	a_2	146
						b_2	142 (8)			b_2	137 (2)
						a_1	132 (2)			a_1	132
						b_1	89 (7)			b_2	77 (2)
						b_2	86 (3)			b_1	70 (3)
						a_2	77 (0)			a_2	65
						a_1	58 (2)			a_1	56 (1)

Table 9. Calculated harmonic frequencies and corresponding IR intensities (in *parentheses*) for the systems studied. In cm^{-1} and km mol^{-1}

trans-UF$_4$(NCS)$_2$		*cis*-UF$_4$(NCS)$_2$		*trans*-UF$_4$(NCO)$_2$		*cis*-UF$_4$(NCO)$_2$		*trans*-UF$_4$(OCN)$_2$		*cis*-UF$_4$(OCN)$_2$	
a_{1g}	1992	a_1	2000 (835)	a_{1g}	2307	a_1	2314 (1308)	a_{1g}	2286	a_1	2292
a_{2u}	1974 (4356)	b_2	1960 (2933)	a_{2u}	2275 (4959)	b_2	2269 (3015)	a_{2u}	2285 (8)	b_2	2285
a_{1g}	968	a_1	973 (3)	a_{1g}	1428	a_1	1431 (63)	a_{1g}	1210	a_1	1207 (54)
a_{2u}	968 (37)	b_2	970 (24)	a_{2u}	1423 (325)	b_2	1420 (196)	a_{2u}	1208 (257)	b_2	1197 (183)
e_u	595 (218)	a_1	603 (317)	e_u	634 (92)	a_1	633 (40)	e_u	612 (215)	a_1	623 (207)
a_{1g}	582	b_1	594 (217)	e_g	632	b_1	633 (90)	a_{1g}	603	b_1	612 (214)
b_{1g}	517 (0)	b_2	557 (127)	e_u	598 (191)	b_2	630 (24)	b_{1g}	531	b_2	580 (124)
e_u	490 (4)	a_1	532 (14)	a_{1g}	592	a_2	629	e_u	518 (24)	a_1	550 (18)
e_g	488	a_1	494 (8)	b_{1g}	520	a_1	610 (217)	e_g	516	b_1	512 (24)
a_{2u}	281 (254)	b_1	489 (4)	a_{2u}	357 (253)	b_1	598 (190)	a_{2u}	362 (132)	a_1	511 (27)
a_{1g}	231	b_2	488	a_{1g}	306	b_2	561 (134)	a_{1g}	315	b_2	511 (3)
b_{2g}	197	a_2	486	e_g	203	a_1	537 (26)	b_{2g}	199	a_2	507
e_g	189	a_1	278 (44)	b_{2g}	197	a_1	351 (54)	e_g	185	a_1	349 (28)
e_u	168 (11)	b_2	252 (114)	e_u	176 (9)	b_2	322 (98)	e_u	169 (7)	b_2	333 (56)
a_{2u}	157 (3)	a_2	196	a_{2u}	170 (6)	a_1	205 (1)	a_{2u}	163 (4)	a_2	196
b_{2u}	121	b_1	194	b_{2u}	132	a_2	203	b_{2u}	124	b_1	192 (3)
e_u	121	a_1	190 (2)	e_u	125	b_1	201	e_u	114	a_1	187 (2)
e_g	29	b_1	167 (12)	e_g	27	b_2	177 (8)	e_g	22	b_2	170 (5)
e_u	14	b_2	167 (6)	e_u	19	b_1	175 (10)	e_u	19 (4)	b_1	163 (6)
		a_1	160 (8)			a_1	170 (9)			a_1	162 (7)
		a_1	122			b_2	130			b_2	122
		b_2	121			a_1	128			a_1	111
		a_2	121			a_2	125			a_2	104
		b_2	36			b_2	32			b_2	28 (2)
		b_1	25			b_1	27			b_1	16 (4)
		a_2	25			a_2	24			a_1	10 (2)
		a_1	15			a_1	20			a_2	i18

3.3.6 Diatomic versus triatomic pseudohalides

Why are the triatomic -NCS and -NCO more stable than -NC? The substantial shortening of the C–O/S distances in -NCS and -NCO suggests a reorganization of the π-electron systems; the π density is moved from the ligand towards the U–X_1 bond. This is accompanied with a shortening of the X_2–X_3 bond distance from 166.9 (122.9) to 157.4 (116.5) pm and an increase of the X_2–X_3 stretching frequencies from 730(1251) in free NCS$^-$(NCO$^-$) to 968(1428 and 1423) cm^{-1} in trans isomers, see Tables 8 and 9. Comparing the natural charges for free and bonded ligands in Table 4 we see that the charge is moved from S to both N and U in the case of –NCS and from both C and O to N and U in the case of –NCO. The –NCS ligand is doing better because its less electronegative sulphur can employ its lone pairs more easily. The NAO populations in Table 3 show that it is mainly the π population of the terminal atom (and the carbon in case of –NCO) which is moved towards X_1 and uranium, and hence to the U–X_1 bond. The σ population is moved to a larger extent only from the X_1 atom. Alternatively, one can speak about delocalization. The –NCS ligand would be best decribed as a mixture of the two Lewis structures $(N=C=S)^-$ and $(N\equiv C\text{-}S)^-$ in Fig. 5. In the bonded ligand, the situation is closer to the first one and in the free ligand to the second one.

From a different point of view, the advantage of the triatomic pseudohalides over diatomic ones could be seen in their mechanical flexibility, the ability to act as a bond-length counterweight, analogous to spin counterweights in catalytical reactions.

The existence of the –CN–U–CN–U–CN– chain species for U(IV) may involve cooperative arrangements of U–N bonds having a dominant π character, and U–C bonds, possibly with more σ character. As neither X-ray crystal structures nor solid-state calculations are available, this awaits a later analysis. For simple, pseudo-octahedral U(VI) molecular models it was found that the sum of energies for *trans*$-UF_4(CN)_2$ and *trans*$-UF_4(NC)_2$ lies only 1.2 kJ/mol higher than twice the energy of the “mixed” *trans*-$UF_4(CN)(NC)$.

3.3.7 The “trans” effect

For complexes of *d* transition metals, the bonds trans to a strong ligand, such as nitride or oxide, tend to be weaker than the cis ones. This is called a trans influence. Denning [48] noted that for the *f* element U(VI), the opposite is true. In for example $[UOCl_5]^-$, the U–Cl bond, trans to the U–O bond, is clearly shorter than the four cis U–Cl bonds. This he termed an inverse trans influence (ITI) and attributed it to 6*p*–5*f* hybridization of the uranium. These two shells have the same parity, and that hybridization leads to an oblate (flattened) charge distribution. In the present case, the differences between cis and trans U–F bond lengths in Table 5 are small, and the point is that none of the present pseudohalides are “strong” ligands, and hence the entire question is not very well defined. O’Grady and Kaltsoyannis [58] considered systems of the type $[MOX_5]^{n-}$ (M = Pa–Np; X = F–Br) and did find the ITI effect.

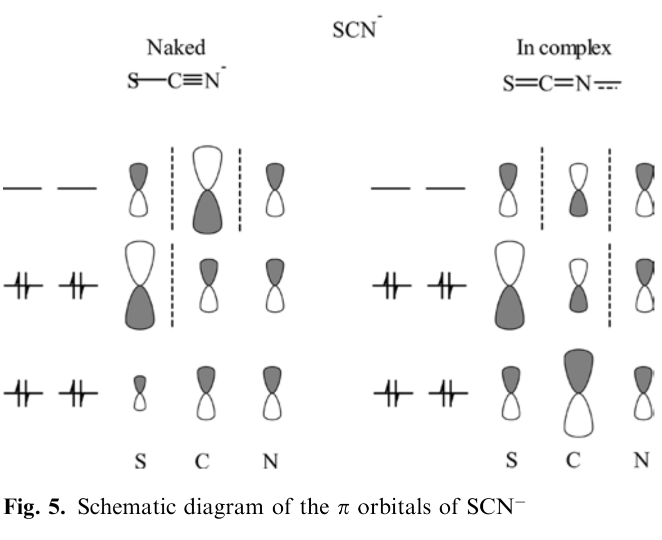

Fig. 5. Schematic diagram of the π orbitals of SCN^-

3.3.8 Covalent radii

provide a further argument that the U–F bond is anomalously short. The covalent radius of fluorine is not well defined [59] but the difference between Pauling’s Cl and F radii would be 99–64 = 35 pm. For the uranium hexahalides, the corresponding difference is of the order of 249-200 = 49 pm. As already discussed, the shortness of the U–F bond can be attributed both to strong electrostatic attraction and to strong covalent bonding, approaching a bond order of 3/2, as symbolically presented in Fig. 2.

The solid UCl_6 contains one nearly octahedral molecule with a U–Cl distance of 247(4) pm and one distorted molecule with three U–Cl a distances of 241(4) pm and three of 251(4) pm [60]. No experimental gas-phase bond length is available for UCl_6. Schreckenbach’s calculated value is 249.4 pm. The experimental UF_6(g) distance is about 200 pm [12].

Concerning the covalent radius of uranium itself, values of 153 and 137 pm were proposed by Pyykkö [61] for U(IV)(coordination number 4) and U(VI)(coordination number 6), respectively, from a fit including even the most electronegative ligands . For the electropositive ligands H_3E(E = Si–Sn), Diaconescu et al. [62] find for U(IV) in $H_3EU(NH_2)_3$ compounds the much larger value of 180 pm.

4 Conclusions

1. There is substantial multiple-bond character in the six bonds of UF_6. The uranium atom acts both as a σ donor and a π acceptor, the fluorine atom as a σ acceptor and a π donor. In addition the bonds are strengthened by ionic contributions.
2. The same is qualitatively true in the uranium–methoxy and other $U(OX)_6$ compounds, and in the uranyl group. These three factors together explain qualitatively the well-known oxophilicity of uranium.
3. In contrast to fluorine, especially the carbon end of –CN is a strong σ donor and a good π acceptor, and hence is an anathema to uranium. Therefore no binary cyanides are known for uranium in any oxidation state. The –NC end is less bad, because it is a better π donor than –CN.
4. The uranium isothiocyanate –NCS (and isocyanate, –NCO) groups suffer an electronic reorganization and corresponding geometry changes from $N\equiv C\text{-}S^-$ towards $N=C=S^-$ upon complexation to U. This improves the $2p\pi$ donor properties of the nitrogen atom.

6. Because the present pseudohalide ligands are not "strong" (such as oxide or nitride), no well-defined trans effects can be discerned in the calculated geometries.

Acknowledgements. This work was supported by The Academy of Finland and the European Research Training Network on "Molecular properties and molecular materials (MOLPROP)", contract no. HPRN-2000-00013. Martin Kaupp is acknowledged for useful discussions and CSC, Espoo, Finland, for computer time on their SGI Origin 2000.

References

1. Slater JL, Sheline RK, Lin KC, Weltner W, Jr (1971) J Chem Phys 55: 5129
2. Zhou MF, Andrews L, Li J, Bursten BE (1999) J Am Chem Soc 121: 9712
3. Kanellakopulos B, Dornberger E, Billich H (1974) J Organomet Chem 76: C42
4. Bagnall KW, Plews MJ, Brown D, Fischer RD, Klähne E, Landgraf GW, Sienel GR (1982) J Chem Soc Dalton Trans : 1999
5. Bagnall KW, Baptista JL (1970) J Inorg Nucl Chem 32: 2283
6. Fischer RD, Sienel GR (1978) J Organomet Chem 156: 383
7. Bonhoure I, Den Auwer C, Cartier dit Moulin C, Moisy P, Berthet JC, Madic C (2000) Can J Chem 78: 1305
8. Hennig H, Rehorek A, Rehorek D, Thomas P (1984) Inorg Chim Acta 86: 41
9. Sles VG, Skoblo AI, Suglobov DN (1974) Radiokhimiya 16: 512
10. Bailey RA, Michelsen TW (1972) J Inorg Nucl Chem 34: 2935
11. del Mar Conejo M, Parry JS, Carmona E, Schultz M, Brennann JG, Beshouri SM, Andersen RA, Rogers RD, Coles S, Hursthouse M (1999) Chem Eur J 5: 3000
12. Weinstock B, Goodman GL (1965) Adv Chem Phys 9: 169
13. Hunt RD, Andrews L, Toth LM (1993) Radiochim Acta 60: 17
14. Gagliardi L, Willetts A, Skylaris CK, Handy NC, Spencer S, Ioannou AG, Simper AM (1998) J Am Chem Soc 120: 11727
15. Schreckenbach G, Hay PJ, Martin RL (1998) Inorg Chem 37: 4442
16. Ismail N, Heully JL, Saue T, Daudey JP, Marsden CJ (1999) Chem Phys Lett 300: 296
17. Schreckenbach G, Hay PJ, Martin RL (1999) J Comput Chem 20: 70
18. Han YK, Hirao K (2000) Chem Phys Lett 324: 453
19. Han YK, Hirao K (2000) J Chem Phys 113: 7345
20. Gagliardi L, Roos BO (2000) Chem Phys Lett 331: 229
21. Gagliardi L, Skylaris CK, Willetts A, Dyke JM, Barone V (2000) Phys Chem Chem Phys 2: 3111
22. Straka M, Dyall KG, Pyykkö P (2001) Theor Chem Acc 106: 393
23. Becke AD (1993) J Chem Phys 98: 5648
24. Lee C, Yang W, Parr RG (1988) Phys Rev B 37: 785
25. Schäfer A, Horn H, Ahlrichs R (1992) J Chem Phys 97: 2571
26. http: //www.theochem.uni-stuttgart.de/pseudopotentiale/
27. Küchle W, Dolg M, Stoll H, Preuss H (1994) J Chem Phys 100: 7535
28. Frisch MJ , Trucks GW, Schlegel HB, Scuseria GE, Robb MA, Cheeseman JR, Zakrzewski VG, Montgomery JA, Stratmann RE, Burant JC, Dapprich S, Millam JM, Daniels AD, Kudin KN, Strain MC, Farkas O, Tomasi J, Barone V, Cossi M, Cammi R, Mennucci B, Pomelli C, Adamo C, Cliord S, Ochterski J, Petersson GA, Ayala PY, Cui Q, Morokuma K, Malick DK, Rabuck AD, Raghavachari K, Foresman JB, Cioslowski J, Ortiz JV, Stefanov BB, Liu G, Liashenko A, Piskorz P, Komaromi I, Gomperts R, Martin RL, Fox DJ, Keith T, Al-Laham MA, Peng CY, Nanayakkara A, Gonzalez C, Challacombe M, Gill PMW, Johnson BG, Chen W, Wong MW, Andres JL, Head-Gordon M, Replogle ES, Pople JA (1998) Gaussian 98, Revision A.7, Gaussian, Pittsburgh, PA
29. Reed AE, Weinstock RB, Weinhold F (1985) J Chem Phys 83: 735
30. te Velde G, Bickelhaupt FM, van Gisbergen SJA, Guerra CF, Baerends EJ, Snijders JG, Ziegler T (2001) J Comput Chem 22: 931
31. Guerra CF, Snijders JG, te Velde G, Baerends EJ (1998) Theor Chem Acc 99: 391
32. Baerends EJ, Autschbach JA, Brces A, Bo C, Boerrigter PM, Cavallo L, Chong DP, Deng L, Dickson RM, Ellis DE, Fan L, Fischer TH, Fonseca Guerra C, van Gisbergen SJA, Groeneveld JA, Gritsenko OV, Grning M, Harris FE, van den Hoek P, Jacobsen H, van Kessel G, Kootstra F, van Lenthe E, Osinga VP, Patchkovskii S, Philipsen PHT, Post D, Pye CC, Ravenek W, Ros P, Schipper PRT, Schreckenbach G, Snijders JG, Sola M, Swart M, Swerhone D, te Velde G, Vernooijs P, Versluis L, Visser O, van Wezenbeek E, Wiesenekker G, Wol SK, Woo TK, Ziegler T ADF2000.02. Theoretical Chemistry, Vrije Universiteit, Amsterdam, The Netherlands, http: //www.scm.com
33. Vosko SH, Wilk L, Nusair M (1980) Can J Phys 58: 1200
34. Perdew JP, et al. (1992) Phys Rev B 46: 6671
35. Ziegler T, Rauk A (1979) Inorg Chem 18: 1558
36. Ziegler T, Rauk A (1979) Inorg Chem 18: 1755
37. Bickelhaupt FM, Baerends EJ (2000) Rev Comput Chem 15: 1
38. Pyykkö P, Li J, Runeberg N (1994) J Phys Chem 98: 4809
39. de Jong WA, Nieuwpoort WC (1996) Int J Quantum Chem 58: 203
40. Hay PJ, Martin RL (1998) J Chem Phys 109: 3875
41. Han YK (2001) J Comput Chem 22: 2010
42. García-Hernandez M, Lauterbach C, Krüger S, Matveev A, Rösch N (2002) J Comput Chem 23: 834
43. Schaftenaar G, Noordik JH (2000) J Comput Aided Mol Des 14: 123
44. Pierloot K (2001) In: Cundari TR (ed), Computational organometallic chemistry. Dekker, New York, pp 123–158
45. Koch W, Frenking G (1985) Chem Phys Lett 114: 178
46. Pyykkö P, Zhao YF (1990) J Phys Chem 94: 7753
47. Bickelhaupt FM, DeKock RL, Baerends EJ (2002) J Am Chem Soc 124: 1500
48. Denning RG (1992) Struct Bonding 79: 215
49. Ohwada K (1976) J Inorg Nucl Chem 38: 741
50. Schreckenbach G (2000) Inorg Chem 39: 1265
51. Templeton LK, Templeton DH, Bartlett N, Seppelt K (1976) Inorg Chem 15: 2720
52. Cuellar EA, Marks TJ (1981) Inorg Chem 20: 2129
53. Heinemann C, Schwarz H (1995) Chem Eur J 1: 7
54. Pyykkö P, Desclaux JP (1978) Chem Phys 34: 261
55. Wang XF, Andrews L (2002) J Am Chem Soc 124: 5636
56. Souter PF, Kushto GP, Andrews L, Neurock M (1997) J Am Chem Soc 119: 1682
57. Golub AM, Köhler H, Skopenko VV (1986) Chemistry of pseudohalides. Elsevier, Amsterdam
58. O'Grady E, Kaltsoyannis N (2002) Dalton Trans : 1233
59. Robinson EA, Johnson SA, Tang TH, Gillespie RJ (1997) Inorg Chem 36: 3022
60. Taylor JC, Wilson PW (1974) Acta Crystallogr B 30: 1481
61. Pyykkö P (1988) Chem Rev 88: 563
62. Diaconescu PL, Odom AL, Cummins TACC (2001) Organometallics 20: 4993
63. Kimura M, Schomaker V, Smith DW, Weinstock B (1968) J Chem Phys 48: 4001
64. Portmann S, Lüthi HP (2000) Chimia 54: 766